# Synthesis and Properties of Functionalized 4 nm Scale Molecular Wires with Thiolated Termini for Self-Assembly onto Metal Surfaces

Changsheng Wang,[†] Martin R. Bryce,*,[†] Joanna Gigon,[‡] Geoffrey J. Ashwell,*,[‡] Iain Grace,[§] and Colin J. Lambert*,[§]

Department of Chemistry, Durham University, Durham DH1 3LE, U.K., The Nanomaterials Group, School of Chemistry, Bangor University, Deiniol Street, Bangor, Gwynedd LL57 2UW, U.K., and Department of Physics, Lancaster University, Lancaster LA1 4YB, U.K.

m.r.bryce@durham.ac.uk; g.j.ashwell@bangor.ac.uk; c.lambert@lancaster.ac.uk

Received January 18, 2008

Core unit with pendant groups to modify HOMO-LUMO levels and electron transport
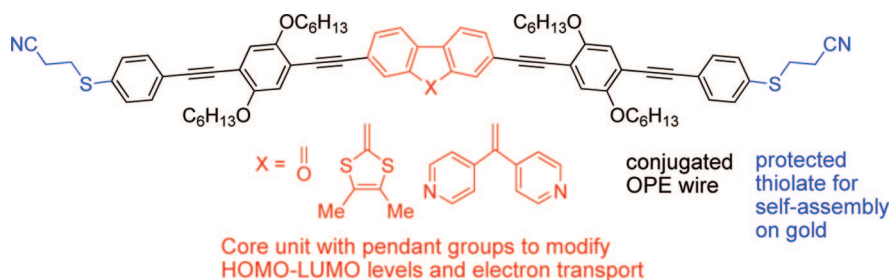
We report the synthesis of new oligo(aryleneethynylene) molecular wires of ca. 4 nm length scale by palladium-catalyzed Sonogashira cross-coupling methodology. Key structural features are the presence of electron donor 9-(1,3-dithiol-2-ylidene)fluorene (compounds **13** and **14**) and electron acceptor 9-[di(4-pyridyl)methylene]fluorene units (compound **16**) at the core of the molecules. Terminal thiolate substituents are protected as cyanoethylsulfanyl (**13** and **16**) or thioacetate derivatives (**14**). The molecules display well-defined redox processes in solution electrochemical studies. The optical properties in solution are similar to those of the fluorenone analog **6**: the strongest absorptions for **6**, **13** and **16** are in the region $\lambda_{max} = 387-393$ nm, with **13** showing an additional shoulder at 415 nm which is not present for **6** and **16**; this shoulder is assigned to a HOMO−LUMO transition from the dithiole to the fluorene unit. Molecules **6**, **13**, **14** and **16** form self-assembled monolayers on gold substrates which exhibit essentially symmetrical current−voltage (*I*−*V*) characteristics when contacted by a gold scanning tunelling microscope (STM) tip. The effects of the chemical modifications at the central unit of **6**, **14** and **16** on the HOMO−LUMO levels and electron transport through the molecules in vacuum have been computed by an ab initio approach.

Introduction

Nanometer-length conjugated organic molecules which can be assembled onto metal or semiconductor surfaces are receiving great attention due to their potential applications as molecular wires in the development of molecular electronics and related fields.[1] A long-term aim of this technology is to overcome the miniaturization threshold of silicon-based devices by utilizing small assemblies of organic molecules, or even single molecules, as components in conductors, rectifiers, switches, transistors, memory elements and logic gates. Developing structure/property relationships in wire-like molecules and probing their self-assembly behavior at the electrode interface are key topics for current investigations. Interconnection of the molecular structure into electronic circuits is usually achieved via terminal thiol-gold contacts.[2] Scanning probe microscopy (SPM), mechanically controllable break junction (MCBJ) and electromigration tech-

[†] Durham University.
[‡] Bangor University.
[§] Lancaster University.

(1) Reviews: (a) Tour, J. M. *Acc. Chem. Res.* **2000**, *33*, 791–804. (b) Carroll, R. L.; Gorman, C. B. *Angew. Chem., Int. Ed.* **2002**, *41*, 4378–4400. (c) Maruccio, G.; R.; Cingolani, R.; Rinaldi, R. *J. Mater. Chem* **2004**, *14*, 542–554. (d) Troisi, A.; Ratner, M. A. *Small* **2006**, *2*, 172–181. (e) James, D. K.; Tour, J. M. *Aldrichimica Acta* **2006**, *39* (2), 47–56. (f) Weibel, N.; Grunder, S.; Mayor, M. *Org. Biomol. Chem.* **2007**, *5*, 2343–2353.

CHART 1. Structures of Functionalized OPE Derivatives Reported Previously
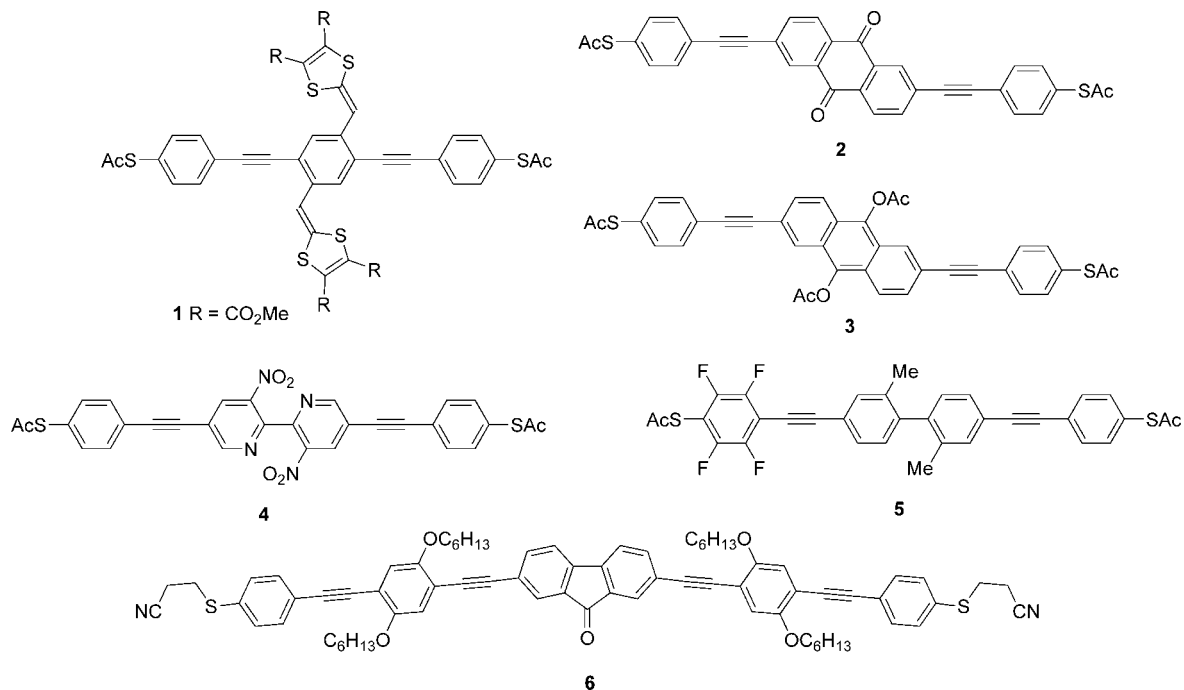
niques have been used for the electrical characterization of the resulting hybrid nanostructures.[3] It is a major challenge to distinguish whether properties arise from the molecule or from the molecule—electrode interface, especially at the single-molecule level.

Efficient electronic communication over nanometer distances requires molecules which possess delocalized π-systems with low HOMO—LUMO gaps. Oligo(aryleneethynylene)s, (aryl-C≡C—)$_n$, are an attractive class of molecules in this regard.[4] They offer the advantages of rigid-rod, length-persistent structures, although it should be noted that the barrier to rotation about the aryl-ethynyl bond is low (typically <1 kcal mol^{-1} for aryl = phenylene, i.e., OPE derivatives),[5] which means that the phenylene rings are freely rotating at room temperature, which will reduce conductance when they are rotated with respect to each other. It has also been proposed that the short ethynyl bond (C≡C length ca. 1.22 Å) in OPE disrupts the conjugation of the backbone more than the vinyl linkage (C=C length ca. 1.35 Å) in OPV [oligo(phenylenevinylene)] systems, i.e., there is increased bond alternation in OPE resulting in a HOMO—LUMO gap larger than that in OPV.[6] Several studies have concerned OPE derivatives with terminal thiol groups[6,7] and some of these molecules have been integrated into an electronic circuit.

Recently, thiol-terminated aryleneethynylenes with more elaborate functionality either in the backbone or as pendant

groups have been synthesized for potential molecular electronics applications. Examples include a derivative with a chiral 1,1′-binaphthyl core,[8] compound **1** with redox activity imparted by pendant 1,3-dithiol-2-ylidene units,[9] and compounds **2** and **3** with cross-conjugated anthraquinone and conjugated anthracene cores, respectively (Chart 1).[10] These molecules show interesting optoelectronic properties in solution, but to the best of our knowledge, their self-assembly and electrical properties in devices have not yet been reported. Compound **4** in a MCBJ device displays voltage-dependent conductance switching which has been used as a single-molecule memory element by reading and erasing bits by simple voltage pulses.[11] Compound **5** is a donor—acceptor system with two weakly coupled π-systems. In a MCBJ device single molecules displayed weak diode-like behavior with a rectification ratio of ca. 1:5 at ±1.5 V.[12] OPE

(2) Love, J. C.; Estroff, L. A.; Kriebel, J. K.; Nuzzo, R. G.; Whitesides, G. *Chem. Rev.* **2005**, *105*, 1103–1169.

(3) (a) James, D. K.; Tour, J. M. *Chem. Mater.* **2004**, *16*, 4423–4435. (b) McCreery, R. L. *Chem. Mater.* **2004**, *16*, 4477–4496. (c) Tao, N. *J. Mater. Chem.* **2005**, *15*, 3260–3263. (d) Lindsay, S. M.; Ratner, M. A. *Adv. Mater.* **2007**, *19*, 23–31. (e) Chen, F.; Hihath, J.; Huang, Z.; Li, X.; Tao, N. J. *Annu. Rev. Phys. Chem.* **2007**, *58*, 535–564.

(4) (a) Bunz, U. H. F. *Chem. Rev.* **2000**, *100*, 1605–1645. (b) Atienza, C.; Martín, N.; Wielopolski, M.; Haworth, N.; Clark, T.; Guldi, D. M. *Chem. Commun.* **2006**, 3202–3204.
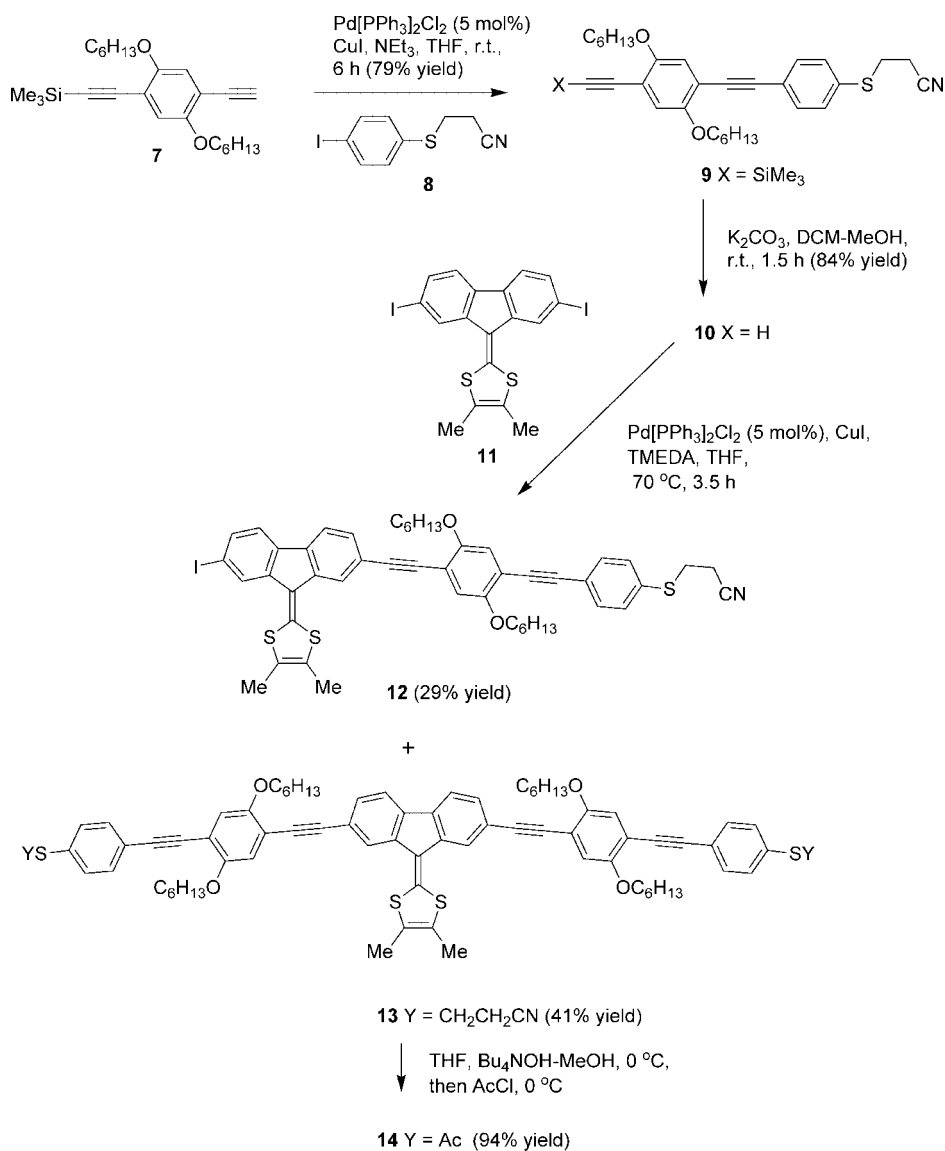
(5) (a) Greaves, S. J.; Flynn, E. L.; Futcher, E. L.; Wrede, E.; Lydon, D. P.; Low, P. J.; Rutter, S. R.; Beeby, A. *J. Phys. Chem. A* **2006**, *110*, 2114–2121. (b) James, P. V.; Sudeep, P. K.; Suresh, C. H.; Thomas, K. G. *J. Phys. Chem. A* **2006**, *110*, 4329–4337.

(6) (a) Kushmerick, J. G.; Holt, D. B.; Pollack, S. K.; Ratner, M. A.; Yang, J. C.; Schull, T. L.; Naciri, J.; Moore, M. H.; Shashidhar, R. *J. Am. Chem. Soc.* **2002**, *124*, 10654–10655. (b) In this communication the OPE and OPV derivatives studied experimentally have different end groups. The OPE has terminal -C$_6$H$_4$-S units, whereas the OPV has terminal -C$_6$H$_4$-CH$_2$-S units. For the OPV with terminal -C$_6$H$_4$-S units, see: Seferos, D. W.; Trammell, S. A.; Bazan, G. C.; Kushmerick, J. G. *Proc. Natl. Acad. Sci. U.S.A.* **2005**, *102*, 8821–8825.

(7) (a) Tour, J. M.; Rawlett, A. M.; Kozaki, M.; Yao, Y. X.; Jagessar, R. C.; Dirk, S. M.; Price, D. W.; Reed, M. A.; Zhou, C. W.; Chen, J.; Wang, W. Y.; Campbell, I. *Chem. Eur. J.* **2001**, *7*, 5118–5134. (b) Mayor, M.; Weber, H. B.; Reichert, J.; Elbing, M.; von Hänisch, C.; Beckmann, D.; Fischer, M. *Angew. Chem., Int. Ed.* **2003**, *42*, 5834–5838. (c) Stuhr-Hansen, N.; Sørensen, J. K.; Moth-Poulsen, K.; Christensen, J. B.; Bjørnholm, T.; Nielsen, M. B. *Tetrahedron* **2005**, *61*, 12288–12295. (d) Haiss, W.; Wang, C.; Grace, I.; Batsanov, A. S.; Schiffrin, D. J.; Higgins, S. J.; Bryce, M. R.; Lambert, C. J.; Nichols, R. J. *Nat. Mater.* **2006**, *5*, 995–1002. (e) Ashwell, G. J.; Urasinska, B.; Wang, C.; Bryce, M. R.; Grace, I.; Lambert, C. J. *Chem. Commun.* **2006**, 4706–4708. (f) Tam, I. W.; Yan, J.; Breslow, R. *Org. Lett.* **2006**, *8*, 183–185. (g) Shi, Z.-F.; Shi;Wang, L.-J.; Wang, H.; Cao, X.-P.; Zhang, H.-L. *Org. Lett.* **2007**, *7*, 595–598. (h) Nilsson, D.; Watcharinyanon, S.; Eng, M.; Li, L.; Moons, E.; Johansson, L. S. O.; Zharnikov, M.; Shaporenko, A.; Albinsson, B.; Mårtensson, J. *Langmuir* **2007**, *23*, 6170–6181. (i) Wang, C.; Batsanov, A. S.; Bryce, M. R.; Ashwell, G. J.; Urasinska, B.; Grace, I.; Lambert, C. J. *Nanotechnology* **2007**, *18*, 044005/1–8. (j) Huber, R.; González, M. T.; Wu, S.; Langer, M.; Grunder, S.; Horhoiu, V.; Mayor, M.; Bryce, M. R.; Wang, C.; Jitchati, R.; Schönenberger, C.; Calame, M. *J. Am. Chem. Soc.* **2008**, *130*, 1080–1084.

(8) Zhu, Y.; Gergel, N.; Majumdar, N.; Harriott, L. R.; Bean, J. C.; Pu, L. *Org. Lett.* **2006**, *8*, 355–358.

SCHEME 1. Synthesis of 13 and 14

In our initial studies we reported the synthesis and solution electrochemistry of the aryleneethynylene derivative **6** with a fluorenone core and a derivative incorporating three fluorenone units (intramolecular S···S distances of ca. 3.7 and 7.0 nm,

respectively.)[15] We subsequently reported the electrical properties of a self-assembled monolayer (SAM) of a 7 nm analog with a central 9-[di(4-pyridyl)methylene]fluorene unit.[7e,i] However, it is experimentally very challenging to make reliable contact to single molecules of lengths greater than ca. 4 nm by scanning probe or break junction techniques, thereby limiting their applications in molecular electronics. The theoretical modeling of longer molecules is also more time-consuming and data are harder to interpret unambiguously. In this regard, molecules of 1−4 nm lengths are more attractive candidates, and we now present the synthesis of the new ca. 4 nm long systems **13**, **14** and **16** with different pendant substituents on the central fluorene unit, namely, 1,3-dithiol-2-ylidene (electron donor) and di(4-pyridyl)methylene (electron acceptor). This strategy offers the possibility of adjusting the energy of the frontier orbitals and hence the HOMO−LUMO gap, as demonstrated previously for nonconjugated (diode-like) structures[16]

(9) Sørensen, J. K.; Vestergaard, M.; Kadziola, A.; Kilså, K.; Nielsen, M. B. *Org. Lett.* **2006**, *8*, 1173–1176.

(10) Van Dijk, E. H.; Myles, D. J. T.; van der Veen, M.; Hummelen, J. C. *Org. Lett.* **2006**, *8*, 2333–2336.

(11) Lörtscher, E.; Ciszek, J. W.; Tour, J.; Riel, H. *Small* **2006**, *2*, 973–977.

(12) Elbing, M.; Ochs, R.; Koentopp, M.; Fischer, M.; von Hänisch, C.; Weigend, F.; Evers, F.; Weber, H. B.; Mayor, M. *Proc. Natl. Acad. Sci. U.S.A.* **2005**, *102*, 8815–8820.
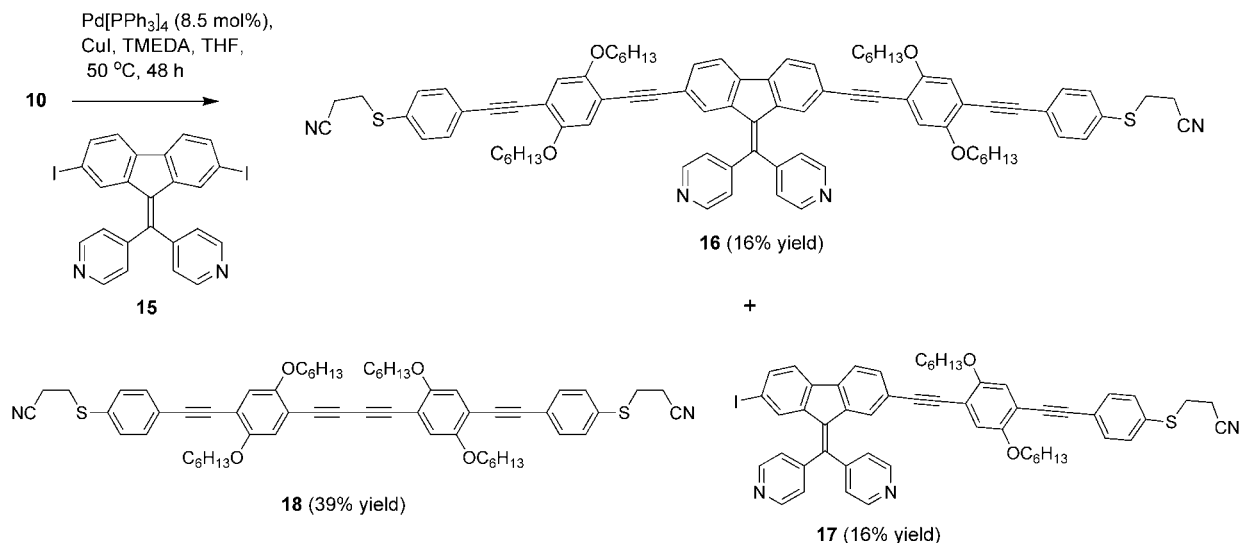
(13) Mayr, A.; Srisailas, M.; Zhao, Q.; Gao, Y.; Hsieh, H.; Hoshmand-Kochi, M.; Fleur, N. S. *Tetrahedron* **2007**, *63*, 8206–8217.

(14) Grunder, S.; Huber, R.; Horhoiu, V.; González, M. T.; Schönenberger, C.; Calame, M.; Mayor, M. *J. Org. Chem.* **2007**, *72*, 8337–8344.

(15) Wang, C.; Batsanov, A. S.; Bryce, M. R.; Sage, I. *Org. Lett.* **2004**, *6*, 2181–2184.

(16) Perepichka, D. F.; Bryce, M. R. *Angew. Chem., Int. Ed.* **2005**, *44*, 5370–5373, and references therein.

SCHEME 2. Synthesis of 16, 17 and 18

FIGURE 1. UV−vis absorption spectra of **6**, **12**, **13** and **16**−**18** in chloroform solution.

and conjugated oligomers.[17] We also report that **6**, **13**, **14** and **16** readily form SAMs on gold substrates which exhibit symmetrical current−voltage (*I*−*V*) characteristics when contacted by a gold scanning tunelling microscope (STM) tip. Furthermore, ab initio calculations for the dithiol derivatives of the series of molecules **6**, **13** and **16** qualitatively support the experimental data and show how the substituents modify the HOMO−LUMO levels; the calculations also reveal that Fano resonances can be controlled by modifying the side group.

Results and Discussion

Synthesis. A key feature of the new molecular wires **13** and **16** is the presence of the central 9-(1,3-dithiol-2-ylidene)fluorene and 9-[di(4-pyridyl)methylene]fluorene units embedded in the backbone which impart redox activity to the molecules (see electrochemical section, below). Protected thiol anchor groups are present at both terminal positions. Our synthetic strategy was similar for both **13** (Scheme 1) and **16** (Scheme 2): compound **10** served in both schemes as the key reagent for 2-fold couplings with the diiodo-derivatives of the core units, viz., compounds **11** and **15**, respectively. This represents a different and more efficient protocol compared with that used in the previous synthesis of **6**.[15]

Reaction of **7**[18] with **8**[7d,19] under standard Sonogashira conditions[20] yielded the cross-coupled product **9** (Scheme 1). The TMS-acetylene unit of **9** was cleanly deprotected to afford the terminal alkyne **10** in the presence of the cyanoethylsulfanyl group, under conditions used previously for analogs of **9**.[18] Reaction of **10** (2.1 equiv) with core reagent **11**[21] gave the monosubstituted product **12** (29% yield) alongside the desired symmetrical product **13** (41% yield) arising from 2-fold
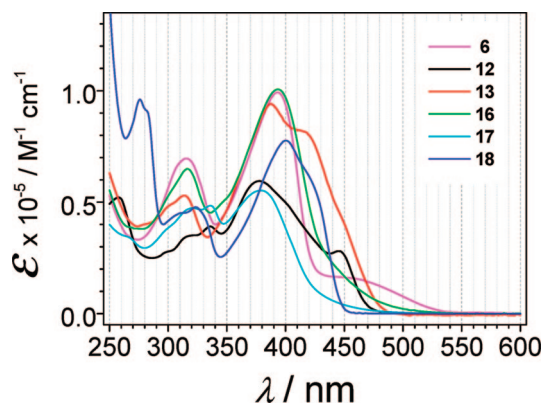
Sonogashira reaction of **11**. The terminal cyanoethylsulfanyl groups of **13** were cleanly converted into the thioacetate groups upon reaction with base and acetyl chloride[7d,19] to give analog **14**.

The synthesis of **16** is outlined in Scheme 2. Compound **15**[18] reacted, as above, with reagent **10** to give the desired product **16** and the monosubstituted partner **17** in equal yields. A significant side reaction on this occasion was oxidative homo-coupling of **10** to give the symmetrical 1,3-butadiyne derivative **18** (39% yield). All three products from the reaction were cleanly separated.

Solution Optical and Electrochemical Properties. The optical properties of the series of compounds **6**, **12**, **13**, and **16**−**18** were studied in chloroform solution (Figure 1). The two distinct bands in the absorption spectra of all of the compounds are consistent with previous data for phenyleneethynylene derivatives possessing dialkoxy substituents which have been assigned to the electronic transitions from nearly identical HOMO and HOMO-1/HOMO-2 to LUMO levels.[5b] A general trend is that similar λ_{max} values are observed for the wires of comparable length, implying that the conjugation pathway along the aryleneethynylene backbone is not disrupted by varying the substituent at C(9) of the central fluorene unit. For compounds **6**, **13** and **16** the strongest absorptions are in the region $\lambda_{max} = 387−393$ nm, with **13** showing an additional shoulder at 415 nm which is not present for **6** and **16**; this shoulder is assigned

(17) (a) Berlin, A.; Zotti, G.; Zecchin, S.; Schiavon, G.; Vercelli, B.; Xanelli, A. *Chem. Mater.* **2004**, *16*, 3667–3676. (b) Zhang, G. L.; Ma, J.; Jiang, Y. S. *Macromolecules* **2003**, *36*, 2130–2140.

(18) Wang, C.; Batsanov, A. S.; Bryce, M. R. *J. Org. Chem.* **2006**, *71*, 108–116.

(19) Synthetic details are given in the supplementary information for ref 7d.

(20) (a) Sonogashira, K. *J. Organomet. Chem.* **2002**, *653*, 46–49. (b) Chinchilla, R.; Nájera, C. *Chem. Rev.* **2007**, *107*, 874–922.

(21) Amriou, S.; Wang, C.; Batsanov, A. S.; Bryce, M. R.; Perepichka, D. F.; Ortí, E.; Viruela, R.; Vidal-Gancedo, J.; Rovira, C. *Chem. Eur. J.* **2006**, *12*, 3389–3400.
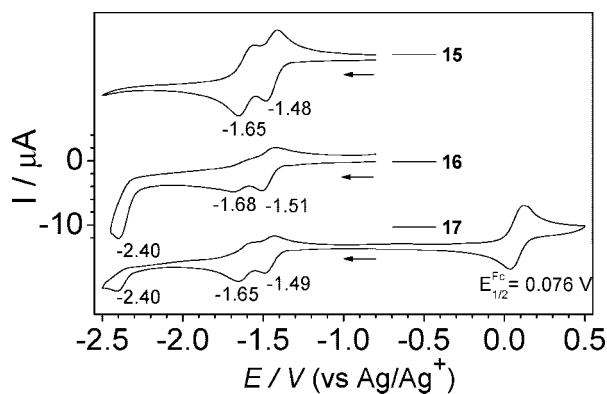
FIGURE 2. CVs of compounds **15**, **16** and **17** in DMF solution containing Bu₄NPF₆ (0.1 M), scan rate 100 mV s⁻¹. E_{red} values are shown for **15**, **16**, and **17**. Ferrocene was added as internal reference to the solution of **17**.

to a HOMO−LUMO transition from the dithiole to the fluorene unit.[21] For the shorter (monocoupled) wires **12** and **17**, the strongest absorptions are blue-shifted to $\lambda_{max} = 377$ and 379 nm, respectively.

Cyclic voltammetry (CV) and differential pulse voltammetry (DPV) studies have probed the redox properties of the wire molecules. We will first consider molecules **6**, **15**, **16** and **17** with electron-acceptor characteristics due to the fluorenone or di(4-pyridyl)methylene-9-fluorene units. We have previously reported[15] that compound **6** displays a reversible single-electron reduction wave at $E_{1/2} = -1.44$ V (in DMF, vs Ag/Ag⁺) when the cathodic scan was limited to −1.8 V. Scanning to more negative potentials revealed two additional irreversible waves at $E_{red} = -2.10$ and −2.23 V, associated with the reduction of the triple bonds. However, after scanning to such negative potentials on the return scan the fluorenone reduction became irreversible, presumably due to a chemical reaction changing the molecular structure.

Figure 2 shows the CVs in DMF solution of **16**, **17** and the central building block **15**. The reduction process for **15** is well-defined: the two, one-electron reduction waves are reversible with potentials at $E_{1/2} = -1.45$ and −1.61 V, yielding the radical anion and dianion species, respectively. This is in excellent agreement with a diethynyl derivative of **15**, which also exhibited two reversible reduction waves.[22] Similar to a 7 nm long analog,[7i] the reduction of **16** gave a quasi-reversible wave at $E_{red} = -1.51$ V (vs Ag/Ag⁺) and an irreversible wave at $E_{red} = -1.68$ V, associated with the reduction of the 9-[di(4-pyridyl)methylene]fluorene unit. However, the second reduction wave of **16** is stronger (increased current) compared with those of longer derivatives. The reduction associated with the triple bonds of **16** appeared as one irreversible peak at $E_{red} = -2.40$ V.

The CV profile for the monocoupled derivative **17** is in between that of **15** (the noncoupled precursor) and **16** (the dicoupled product). The second reduction wave of **17** ($E_{red} = -1.65$ V) is stronger on both the cathodic and anodic scans, although the wave is still not reversible. However, the relative intensity of the acetylenic reduction at −2.40 V decreased compared to **16**, agreeing with this wave arising from the phenyleneethynylene (PE) sidearm(s) in **16** and **17**. It seems clear that the PE side-arms are responsible for the reduced reversibility of the electrochemistry of the molecular wire **16**.
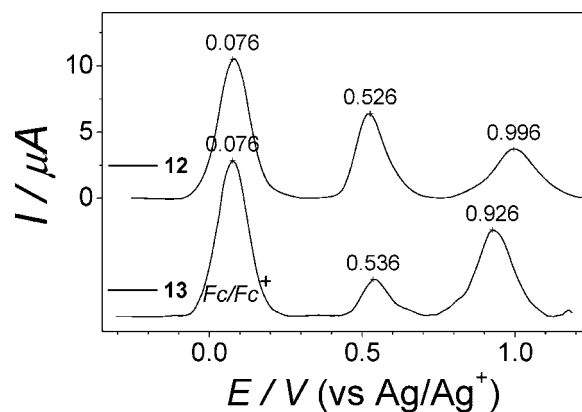
(22) Wang, C.; Batsanov, A. S.; Bryce, M. R. *Faraday Discuss.* **2006**, *131*, 221–234.

FIGURE 3. Differential pulse voltammograms of compounds **12** and **13** in DMF solution containing Bu₄NPF₆ (0.1 M), scan rate 100 mV s⁻¹. Ferrocene was added as internal reference to the solutions.

The reduction waves of the 9-[di(4-pyridyl)methylene]fluorene unit in **16** showed solvent dependence. The second reduction peak increased in intensity in THF compared to DMF, although the reversibility was not improved (see Supporting Information, Figure S1). Varying the scan rate (50−1600 mV s⁻¹) did not change the quasi-reversibility of the reductions. The CVs of **17** obtained in THF at different scan speeds are shown in Supporting Information (Figure S2). The relative intensity of the second reduction wave on the reversed cathodic scans remained unchanged at the different scan rates, which suggests that the reductive electrochemical process of these wire compounds is not kinetically controlled.

In contrast to the electron-accepting central units in the wires **6**, **16** and **17**, the 1,3-dithiol-2-ylidene unit imparted good electron donor characteristics to molecules **12**, **13** and **14**. The data for **13** and **14** were identical within experimental error, showing that the protecting groups have no effect on the redox chemistry. The DPVs of compounds **12** and **13** are shown in Figure 3. (For these compounds DPV was preferable to CV due to their limited solubility.) When the anodic scans were limited to 0.8 V, a reversible oxidation wave corresponding to radical cation formation was observed at ca. 0.53 V for both compounds. (Reversibility was established in CV experiments.) A second irreversible oxidation process, assigned to dication formation was observed at 0.93−1.0 V: the potential for this wave is positively shifted by 70 mV for **12** compared to **13** due either to the presence of the electron-withdrawing iodine substituent in **12** or the extended conjugation in **13** stabilizing its dication, which is a well-known phenomenon for π-extended tetrathiafulvalenes. The first oxidation wave of **12** and **13** became irreversible when the anodic scans were extended beyond 0.8 V, indicating decomposition of the dications. The CVs of compounds **11**−**14** are shown in Supporting Information.

Self-Assembly and Electrical Characterization. To establish the potential of these molecules as candidates in electrical circuits, we have investigated their self-assembly on gold-coated substrates and performed preliminary STM experiments on the resultant monolayer structures. We focus on the electrical characterization of monolayers formed from **13** (cyanoethyl-protected) and **14** (acetyl-protected); they were assembled under mildly basic conditions, using sodium methoxide and ammonia, respectively, to remove the protecting groups, and the process was monitored from the frequency changes following deposition on gold-coated 10 MHz quartz crystals. The plasma-cleaned substrates were repeatedly immersed for 10−15 min intervals
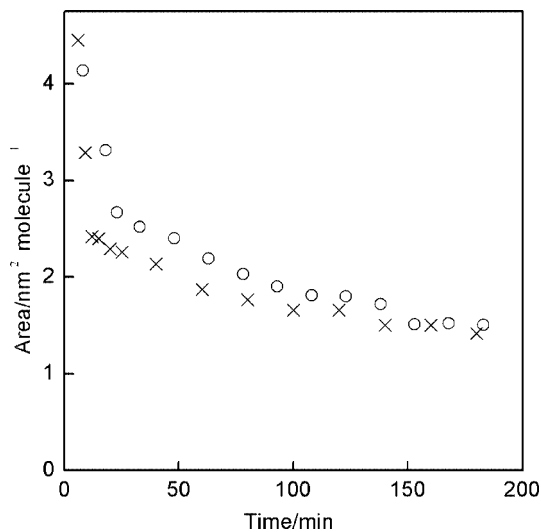
FIGURE 4. Variation of the mean molecular area versus the total period of immersion of gold-coated 10 MHz quartz crystals in a THF solution of **14** (0.1 mg/mL) with (×) and without (○) addition of 2 drops of ammonia solution.

FIGURE 5. $I-V$ characteristics of SAMs of **14** formed under basic conditions on gold contacted by a gold probe. The data were obtained by averaging 10 scans on the same site for a set point current of 200 pA and bias of $+0.2$ V where the polarity is defined by the sign of the substrate electrode.

in basic tetrahydrofuran solutions of the wires (0.1 mg mL^{-1}) and thoroughly rinsed each time to remove any physisorbed material. The frequency saturated to a constant value after ca. 2 h, and a Sauerbrey analysis[23] of the data yielded areas of 1.2−1.5 nm^2 molecule^{-1}, which is consistent with the area calculated from van der Waals' dimensions of the chemisorbed molecular wire assuming partial overlap of these tilted molecules in the SAM. We note that assembly also occurs spontaneously without the need for added base, and similar data have been obtained for **14** in the absence of ammonia (Figure 4). The deposition time is similar under both sets of conditions. The areas were calculated for the molecular mass, and values at saturation are consistent with those from molecular modeling. It is, therefore, confidently assumed that deposition occurs to give monolayers without the formation of disulfides, which would significantly reduce the calculated area.

For the electrical characterization of **13** and **14** the self-assembled monolayers (SAMs) were formed under basic conditions to ensure removal of the protecting groups at both termini, which if retained could act as a barrier to conduction. SAMs on gold-coated highly oriented pyrolytic graphite (HOPG) were investigated by scanning tunneling spectroscopy using a range of set-point conditions to land the gold probe. The set-point current and voltage have minimal effect on the profile of the current−voltage ($I-V$) curves but affect the magnitude of the tunneling current by influencing the distance between probe and surface. Symmetrical or almost symmetrical $I-V$ characteristics have been obtained (Figure 5), this being expected from these wire-like molecules, but slight electrical asymmetry is induced for the more extreme set-point conditions.

SAMs were also investigated by the "current-jump" technique of Haiss et al.[24] Studies were performed with the gold probe located at a fixed height above the surface and as the current was monitored as a function of time. Films of the molecular wires showed abrupt changes in current (Figure 6). These events persist for ca. 50−100 ms with 30% of all jumps corresponding to 0.12 ± 0.03 nA at 300 mV, this also being the lowest
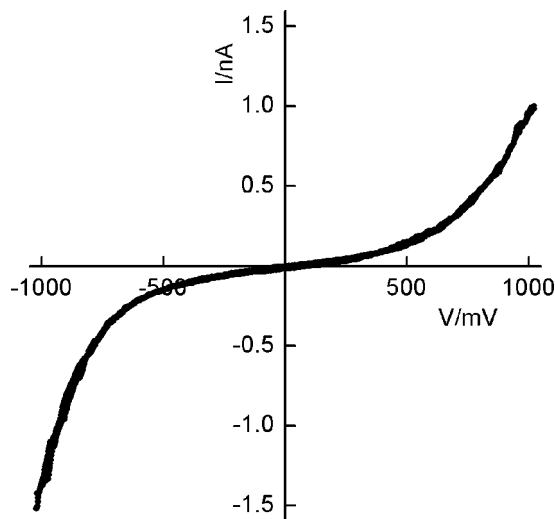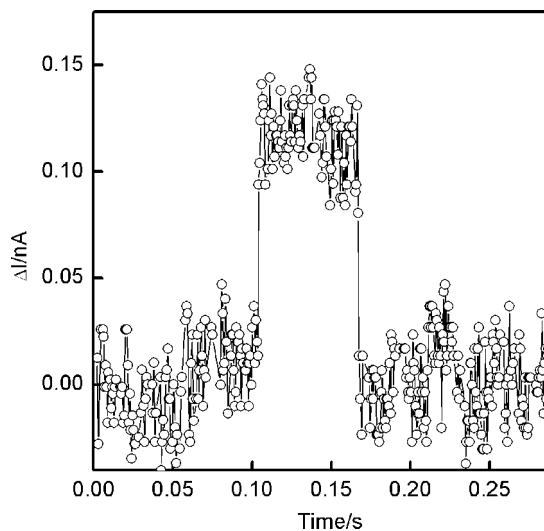

FIGURE 6. Characteristic current jump obtained with a gold STM probe located at a fixed height above a SAM of **14** at a bias at 300 mV. (The SAM was formed under basic conditions.)

observed current. The SAMs formed from **6** and **16** also exhibit essentially symmetrical $I-V$ curves as shown in Supporting Information. The general shapes of the curves show some differences which may be induced by different tip distances above the monolayer surfaces as well as by the different molecules being contacted. Sixty percent of the current jumps of the SAMs from **6** and **16** measured at 300 mV were 0.10 ± 0.05 nA and 0.17 ± 0.05 nA, respectively. Such behavior is consistent with the formation of short-lived contacts between the Au probe and the organic monolayer. The measured current jumps are normally associated with a single-molecule event,[24] although for molecules of this length it is unlikely that Au-S contacts have been established between the probe and SAM. Thus, the current jumps may not relate to the current along the entire Au-S−wire−S-Au length but from contact via the gold probe to the body of the chromophore which is tilted toward the substrate with an Au−S−C angle of ca. 30°. The differences in the HOMO and LUMO levels calculated for the series **6, 14**

(23) Sauerbrey, G. *Z. Phys.* **1959**, *155*, 206–222.
(24) Haiss, W.; Nichols, R. J.; van Zalinge, H.; Higgins, S. J.; Bethell, D.; Schiffrin, D. J. *Phys. Chem. Chem. Phys.* **2004**, *6*, 4330–4337.
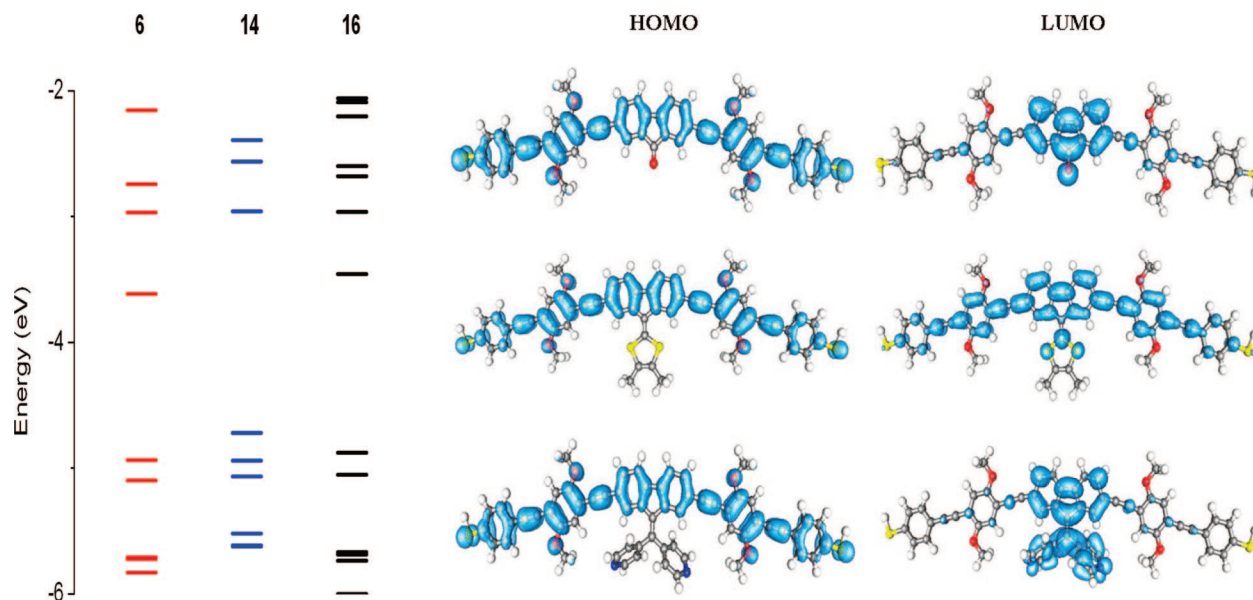
FIGURE 7. (Left) Energy levels of the isolated dithiol derivatives of molecule **6**, **14**, and **16**. (Right) The spatial distribution of the HOMO and LUMO orbitals for **6** (top) **14** (middle) and **16** (bottom) (with methoxy groups replacing the hexyloxy side chains).

and **16** (see below) did not give rise to any significant trends in the experimental $I-V$ profiles. Nonetheless, to have established that this series of molecules which incorporate a significant level of functionality can be self-assembled on gold and conductance data can be obtained is an important first step in using these molecules in electrical circuits.

Theoretical Studies. To probe the electronic properties of **6**, **14** and **16**, the HOMO—LUMO levels and electron transport through the molecules in vacuum have been computed by an ab initio approach, using a combination of the density functional theory (DFT) code SIESTA[25] and a Green's function scattering approach, as encapsulated in the nonequilibrium molecular electronics SMEAGOL code.[26] Studying trends and making comparisons between the types of orbitals displayed within a series of molecules can provide a qualitative understanding of the experimentally observed behavior. From a theoretical viewpoint the series **6**, **14** and **16** are appealing systems where different side groups have been chemically engineered into the central unit of the molecules. The electron transport in many molecular devices is dominated by conduction through broadened HOMO or LUMO states leading to Breit—Wigner resonances.[27]

Figure 7 presents the electronic properties of the series of molecules **6**, **14** and **16** (with methoxy groups replacing the hexyloxy side chains); the level structure shows how the HOMO—LUMO gap is modified by altering the side groups on the central unit. Compounds **6** and **16** have values of ca. 1.4 eV, whereas **14** is slightly larger at ca. 1.7 eV. The spatial distribution of the HOMO orbital is very similar for each molecule with this orbital delocalized along the backbone of the molecule. The main difference occurs in the LUMO orbital: for **6** and **16** it is localized on the central unit, whereas the LUMO of **14** is delocalized. Compounds **6** and **16** have lower lying LUMOs than **14**, which is consistent with their stronger electron accepting properties. Compound **14** has the highest lying HOMO in the series, consistent with the electron-donating properties imparted by the dithiole

substituent. These data are qualitatively consistent with the solution electrochemical properties discussed above.

To calculate the transport properties of these molecules, they were attached to gold leads; the zero bias transmission coefficients are shown in Figure 8. For all three molecules the Fermi energy (0 eV) lies closer to the HOMO resonance, and the magnitude of the conductance is of the order 1−10 nS for all three molecules, which broadly agrees with the STM measurements which show similar conductance values for **6**, **14** and **16**. The main change in the magnitude occurs due to the decrease in the gap between the HOMO and LUMO resonances. The LUMO resonance for **6** and **16** displays a line shape typical of a Fano resonance,[28] with a resonance accompanied by an antiresonance at ca. 1 eV, while the LUMO of **14** shows a typical Breit—Wigner resonance. For **14** a Fano resonance occurs at higher energy at ca. 1.8 eV. This behavior can be attributed to the spatial distribution of the orbitals displayed in Figure 7, with a Fano resonance occurring when the orbital is *localized* on the central unit and pendant group of the molecule (compounds **6** and **16**). The Fano resonance is due to interference between a bound state on the side group and the molecular backbone. A Breit—Wigner resonance, on the other hand, arises when an orbital is *delocalized* along the backbone of the molecule, as seen for compound **14**.

This behavior in the series **6**, **14** and **16** opens up the possibility of controlling transport through such molecules, since Fano resonances are sensitive to geometrical and chemical changes to the central and pendant groups.[29] This sensitivity, which is not present in Breit—Wigner resonances, suggest that such structures, especially **6** and **16**, could be used as future single-molecule chemical sensors. To observe a dramatic change in the conduction would require a change in the properties of the side group causing the Fano resonance to shift closer to the Fermi energy. This could be achieved by geometrical manipulation which affected the conjugation or by a chemical change such as protonation.

(25) Soler, J. M.; Artacho, E.; Gale, J. D.; Garcia, A.; Junquera, J.; Ordejon, P.; Sanchez-Portal, D. *J. Phys.: Condens. Matter* **2002**, *14*, 2745–2779.
(26) Rocha, A. R.; Garcia-Suarez, V.; Bailey, S. W.; Lambert, C. J.; Ferrer, J.; Sanvito, S. *Phys. Rev. B* **2006**, *73*, 085414.
(27) Breit, G.; Wigner, E. *Phys. Rev.* **1936**, *49*, 519–531.

(28) Fano, U. *Phys. Rev.* **1961**, *49*, 1866–1878.
(29) Papadopoulos, T. A.; Grace, I. M.; Lambert, C. J. *Phys. Rev. B* **2006**, *74*, 193306.
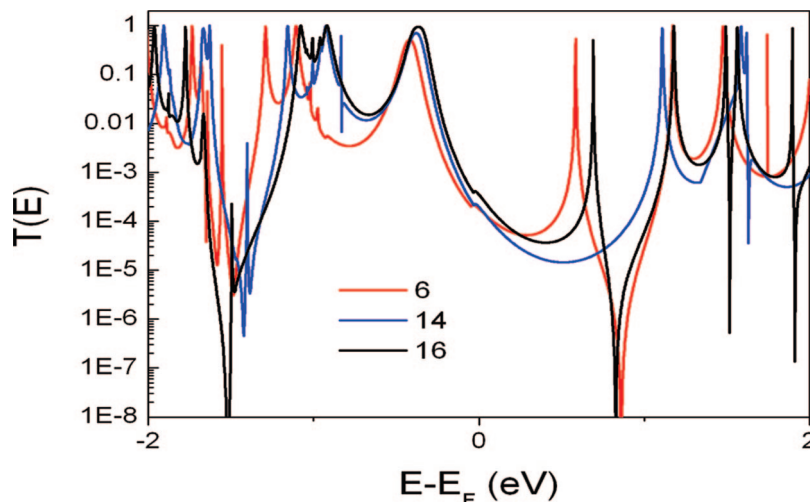
FIGURE 8. Zero bias transmission through dithiol derivatives of molecules **6**, **14**, and **16**.

Conclusions

We have synthesized a series of oligo(aryleneethynylene) molecular wires of ca. 4 nm length scale which are endowed with functional groups at their cores and thiolated terminal substituents. Their optoelectronic properties in solution have been characterized. Systems **6**, **13**, **14** and **16** form self-assembled monolayers on gold substrates which exhibit essentially symmetrical current−voltage (*I*−*V*) characteristics when contacted by a gold scanning tunelling microscope (STM) tip. This is an important first step in using these molecules in electrical circuits. The central fluorenone, 9-(1,3-dithiol-2-ylidene)fluorene and 9-[di(4-pyridyl)methylene]fluorene units modify the HOMO−LUMO levels of the molecules. The spatial distribution of the HOMO orbital is very similar for each molecule with this orbital delocalized along the backbone of the molecule. The main difference occurs in the LUMO orbital: for **6** and **16** it is localized on the central unit, whereas the LUMO of **14** is delocalized.

Future work, which is beyond the scope of this article, will follow two themes. (i) Integrating these oligo(aryleneethynylene) derivatives into a device architecture (e.g., a mechanically controllable break junction) and then applying a bias voltage to electrochemically charge the redox subunit may provide a means of bringing molecular energy states into resonance with the Fermi levels of the electrodes. If this process is reversible, an electrochemically driven conductance switch is obtained. However, these are very intricate experiments, especially at a single-molecule level and only a few experimental demonstrations of this behavior have been reported.[11,12,30] Different adsorption geometries, desorption of the thiol from the gold surface and thermal fluctuations can be induced by an applied bias; all these factors complicate the interpretation of results. (ii) Ab initio calculations have shown that the functional groups in **6**, **14** and **16** impart interesting resonant features which may open the possibility of single-molecule sensing. Compounds **6** and **16**, for which the LUMO resonance displays a

line shape typical of a Fano resonance, are potential candidates in this regard. Attempts to experimentally demonstrate sensing of analytes using these features as the read-out signal will also be undertaken. Protonation of the pyridyl units of **16** is an attractive proposition for sensing.

Experimental Section

General. Details of equipment and procedures are the same as reported previously.[15,18] Pd[PPh₃]₂Cl₂[31] and Pd[PPh₃]₄[32] were prepared by reported methods. *N,N,N′,N′*-Tetramethylethylenediamine (TMEDA) was distilled over sodium metal under argon.

1-[4-(2-Cyanoethylsulfanyl)phenylethynyl]-2,5-dihexyloxy-4-trimethylsilylethynylbenzene (9). To the solution of **8**[7d,19] (1.01 g, 3.49 mmol) in dry THF (20 mL) were added Pd[PPh₃]₂Cl₂ (120 mg, 5 mol%), CuI (40 mg) and triethylamine (80 mL). The mixture was stirred at room temperature for 5 min followed by the addition of **7**[18] (1.40 g, 3.51 mmol) in one portion. The mixture was stirred at room temperature for 6 h to afford a yellow suspension. The solid was removed by suction filtration, and the filtrate was dried by vacuum evaporation. The dark yellow solid residue was then column chromatographed (silica gel, chloroform) and crystallized from ethanol to afford **9** as yellow crystals (1.54 g, 79%): mp 91.3−92.3 °C; ^{1}H NMR (400 MHz, CDCl₃) δ 7.45 (d, J = 8.4 Hz, 2H), 7.35 (d, J = 8.4 Hz, 2H), 6.95 (s, 1H), 6.94 (s, 1H), 3.98 (m, 4H), 3.17 (t, J = 7.2 Hz, 2H), 2.62 (t, J = 7.2 Hz, 2H), 1.81 (m, 4H), 1.52 (m, 4H), 1.34 (m 8H), 0.90 (m, 6H), 0.26 (s, 9H); ^{13}C NMR (100 Hz, CDCl₃) δ 154.2, 153.5, 133.7, 132.3, 130.4, 122.7, 117.7, 117.3, 116.9, 114.1, 113.8, 101.1, 100.3, 93.9, 87.2, 69.57, 69.54, 31.59, 31.54 29.8, 29.27, 29.23, 25.7, 22.6, 18.2, 14.1, 14.0, −0.1. MS (EI) (*m/z*): 559.1 (M⁺, 100%). Anal. Calcd for C₃₄H₄₅NO₂SSi: C, 72.94; H, 8.10; N, 2.50. Found: C, 72.77; H, 8.08; N, 2.36.

4-[4-(2-Cyanoethylsulfanyl)phenylethynyl]-2,5-dihexyloxy-1-ethynylbenzene (10). To a stirred solution of **9** (1.54 g, 2.75 mmol) in dry DCM (50 mL) was added potassium carbonate powder (0.5 g) followed by methanol (30 mL) using a syringe. The mixture was stirred for an additional 1.5 h and then suction filtered to remove the solid K₂CO₃. Acetic acid (2 mL) was added to the filtrate, and the mixture was evaporated under vacuum to yield a yellow waxy solid, which was purified by column chromatography (silica, chloroform) and recrystallization from methanol to afford

(30) (a) Haiss, W.; Van Zalinge, H.; Higgins, S. J.; Bethell, D.; Hörbenreich, H.; Schiffrin, D. J.; Nichols, R. J. *J. Am. Chem. Soc.* **2003**, *125*, 15294–15295. (b) Kubatkin, S.; Danilov, A.; Hjort, M.; Cornil, J.; Brédas, J. L.; Suhr-Hansen, N.; Hedegård, P.; Bjørnholm, T. *Nature* **2003**, *425*, 698–701. (c) Xu, B.; Xiao, X.; Yang, X.; Zang, L.; Tao, N. *J. Am. Chem. Soc.* **2005**, *127*, 2386–2387. (d) Li, Z.; Pobelov, I.; Han, B.; Wandlowski, T.; Blaszcyk, A.; Mayor, M. *Nanotechnology* **2007**, *18*, 044018. (e) Giacalone, F.; Herranz, M. A.; Grüter, L.; González, M. T.; Calame, M.; Schönenberger, C.; Arroyo, C. R.; Rubio-Bollinger, G.; Vélez, M.; Agraït, N.; Martín, N. *Chem. Commun.* **2007**, 4854–4856.

(31) Heck, R. F. *Palladium Reagents in Organic Synthesis*; Academic Press: London, 1985; p 18.

(32) Hegedus, L. S. In *Organometallics in Synthesis*; Schlosser, M., Ed.; John Wiley & Sons: Chichester, 1994; p 448.

10 as a pale yellow solid (1.13 g, 84%): mp 64.5−66.0 °C; ^{1}H NMR (300 MHz, CDCl$_3$) δ 7.45 (d, J = 8.5 Hz, 2H), 7.32 (d, J = 8.5 Hz, 2H), 6.97 (s, 1H), 6.96 (s, 1H), 3.96 (m 4H), 3.36 (s, 1H), 3.11 (t, J = 7.3 Hz, 2H), 2.58 (t, J = 7.2 Hz, 2H), 1.78 (m, 4H), 1.47 (m, 4H), 1.32 (m, 8H), 0.88 (m, 6H); ^{13}C NMR (75 Hz, CDCl$_3$) δ 153.9, 153.2, 133.8, 132.0, 129.9, 122.2, 117.6, 117.4, 116.5, 114.0, 112.6, 93.9, 86.8, 82.4, 79.8, 69.4, 69.3, 31.35, 31.30, 29.4, 29.0, 28.9, 25.5, 25.4, 22.42, 22.37, 17.9, 13.85, 13.84. MS (EI) (m/z): 487.2 (M$^+$, 100%). Anal. Calcd for C$_{31}$H$_{37}$NO$_2$S: C, 76.35; H, 7.65; N, 2.87. Found: C, 76.29; H, 7.70; N, 2.66.

Compounds 12 and 13. To a suspension of compound **11**[21] (175 mg, 0.32 mmol) in THF (20 mL) and TMEDA (20 mL) were added Pd[PPh$_3$]$_2$Cl$_2$ (22 mg, 5 mol%) and CuI (8 mg), and the mixture was stirred at room temperature for 5 min and then heated and stirred in an oil bath at 70 °C, and compound **10** (0.320 g, 0.656 mmol) was added. These conditions were maintained for 3.5 h to obtain a clear yellow solution which then turned gradually into a yellow suspension after an additional 1 h of stirring. The solvents were removed in vacuo, and the residue was boiled with ethanol (50 mL) for 5 min and then suction filtered to afford an orange-yellow solid which was columned chromatographed on silica (eluted with chloroform) to yield two fractions. The first fraction was crystallized from chloroform−ethanol to yield **12** as a yellow solid (85 mg, 29%): mp 173.8−175.1 °C; ^{1}H NMR (300 MHz, CDCl$_3$) δ 8.10 (s, 1H), 7.96 (s, 1H), 7.79 (d, J = 7.9 Hz, 1H), 7.62 (d, J = 8.1 Hz, 1H), 7.57 (d, J = 7.9 Hz, 1H), 7.50 (d, J = 8.4 Hz, 2H), 7.48 (d, J = 7.8 Hz, 1H), 7.37 (d, J = 8.5 Hz, 2H), 7.09 (s, 1H), 7.03 (s, 1H), 4.07 (t, J = 6.5 Hz, 4H), 3.17 (t, J = 7.3 Hz, 2H), 2.63 (t, J = 7.3 Hz, 2H), 2.20 (s, 6H), 1.89 (m, 4H), 1.57 (m, 4H), 1.36 (m, 8H), 0.89 (m, 6H); ^{13}C NMR (75 Hz, CDCl$_3$) δ 153.7, 153.6, 136.2, 135.9, 133.6, 133.3, 132.3, 131.3, 130.4, 128.3, 125.5, 124.3, 122.7, 121.7, 121.2, 119.4, 117.8, 116.9, 116.8, 114.6, 113.3, 96.7, 93.9, 92.3, 87.4, 85.8, 69.63, 69.58, 31.59, 31.56, 29.8, 29.3, 25.7, 22.7, 18.2, 14.1, 13.1; λ$_{max}$ (CHCl$_3$) 258, 336, 377, 455 nm. MS (MALDI-TOF) (m/z): 905.2 (M$^+$). Anal. Calcd for C$_{49}$H$_{48}$INO$_2$S$_3$: C, 64.96; H, 5.34; N, 1.55. Found: C, 65.04; H, 5.35; N, 1.57.

The second fraction from the column was a mixture containing compound **13** and the self-coupled product **18**. Recrystallizing this mixture from chloroform-toluene then from *p*-xylene gave **13** as a yellow-orange solid (166 mg, 41%): mp 184.7−185.8 °C; ^{1}H NMR (300 MHz, CDCl$_3$) δ 8.01 (s, 1H), 7.82 (d, J = 7.9 Hz, 1H), 7.51 (d, J = 7.9 Hz, 1H), 7.50 (d, J = 8.4 Hz, 2H), 7.36 (d, J = 8.4 Hz, 2H), 7.10 (s, 1H), 7.03 (s, 1H), 4.06 (m, 4H), 3.17 (t, J = 7.3 Hz, 2H), 2.63 (t, J = 7.3 Hz, 2H), 2.20 (s, 3H), 1.89 (m, 4H), 1.57 (m, 4H), 1.37 (m, 8H), 0.90 (m, 6H); ^{13}C NMR (75 Hz, CDCl$_3$) δ 153.7, 153.6, 137.4, 136.6, 133.7, 132.3, 130.4, 128.9, 128.4, 125.6, 124.2, 122.7, 121.6, 119.7, 117.8, 116.9, 116.8, 114.6, 113.3, 96.7, 93.9, 87.4, 85.9, 69.64, 69.57, 31.6, 29.7, 29.3, 25.7, 22.7, 18.2, 14.1, 13.1; λ$_{max}$ (CHCl$_3$) 314, 387, 415(shoulder) nm. MS (MALDI-TOF) (m/z): 1264.6 (M$^+$). Anal. Calcd for C$_{80}$H$_{84}$N$_2$O$_4$S$_4$: C, 75.91; H, 6.69; N, 2.21. Found: C, 75.86; H, 6.73; N, 2.27.

Compound 14. A solution of compound **13** (58 mg, 0.046 mmol) in dry THF (20 mL) was cooled to −2 °C with an acetone−ice bath. Tetrabutylammonium hydroxide solution (1.0 M in methanol, 0.1 mmol) was syringed dropwise under argon atmosphere to afford a clear red-orange solution. Acetyl chloride (0.5 mL) was added, and the resultant clear yellow solution was stirred at 0 °C for 5 min. The solvents were removed in vacuo and the yellow solid residue was column chromatographed (silica, 1:1 DCM−chloroform) to yield **14** as a yellow solid (54 mg, 94%): mp 182.4−185.0 °C; ^{1}H NMR (300 MHz, CDCl$_3$) δ 8.02 (s, 1H), 7.82 (d, J = 7.9 Hz, 1H), 7.57 (d, J = 7.9 Hz, 2H), 7.51 (d, J = 7.9 Hz, 1H), 7.41 (d, J = 7.9 Hz, 2H), 7.10 (s, 1H), 7.04 (s, 1H), 7.09 (m, 4H), 2.44 (s, 3H), 2.22 (s, 3H), 1.90 (m, 4H), 1.58 (m, 4H), 1.39 (s, 8H), 0.90 (m, 6H); ^{13}C NMR (75 Hz, CDCl$_3$) δ 193.13, 154.1, 153.9, 142.7, 137.6, 136.8, 134.1, 132.1, 128.5, 128.2, 125.7, 124.9, 124.2, 121.9, 119.7, 117.6, 117.4, 117.3, 115.2, 96.8, 94.0, 88.0, 86.1, 70.1, 70.0,

31.6, 30.2, 29.5, 25.8, 22.6, 14.0, 13.1. MS (MALDI-TOF) (m/z): 1242.6 (M$^+$). Anal. Calcd for C$_{78}$H$_{82}$O$_6$S$_4$: C, 75.32; H, 6.65. Found: C, 75.20; H, 6.68.

Compounds 16−18. To the solution of compound **15**[18] (117 mg, 0.2 mmol) in dry THF (20 mL) were added Pd[PPh$_3$]$_4$ (25 mg, 8.5 mol%), CuI (10 mg) and TMEDA (10 mL). The mixture was stirred at room temperature for 5 min to afford a clear yellow solution. A solution of compound **10** (205 mg, 0.42 mmol) in THF (10 mL) was added dropwise at 50 °C under Ar. The mixture was continuously heated and stirred for 48 h. The mixture was evaporated in vacuo, and the residue was column chromatographed on a silica column. Using hexane−DCM (1:9 v/v) as eluent yielded compound **18** (79 mg, 39%, based on **10**). Subsequent elution with DCM−diethyl ether (4:1 v/v) afforded **16** (42 mg, 16%, based on **15**) followed by **17** (31 mg, 16%, based on **15**).

16: an orange oil which solidified into a yellow solid upon adding hexane into its toluene solution; mp 119.6−120.8 °C; ^{1}H NMR (400 MHz, CDCl$_3$) δ 8.76 (d, J = 4.6 Hz, 2H), 7.66 (d, J = 7.8 Hz, 2H), 7.49 (m, 3H), 7.36 (d, J = 7.3 Hz, 2H), 7.33 (d, J = 5.8 Hz, 2H), 6.97 (s, 1H), 6.91 (s, 1H), 6.84 (s, 1H), 4.01 (m, 4H), 3.16 (t, J = 7.2 Hz, 2H), 2.62 (t, J = 7.3 Hz, 2H), 1.83 (m, 4H), 1.53 (m, 4H), 1.36 (m, 8H), 0.90 (t, J = 6.7 Hz, 6H); ^{13}C NMR (100 Hz, CDCl$_3$) δ 153.7, 153.6, 150.9, 148.8, 140.2, 139.4, 137.6, 135.3, 133.7, 132.9, 132.3, 130.4, 127.8, 124.0, 122.7, 122.3, 119.8, 117.7, 116.9, 114.0, 113.7, 95.1, 94.0, 87.6, 86.8, 69.7, 69.6, 31.6, 29.8, 29.3, 29.2, 25.72, 25.66, 22.6, 18.2, 14.0; λ$_{max}$ (CHCl$_3$) 316, 393 nm; MS (MALDI-TOF) (m/z): 1302.7 (M$^+$). Anal. Calcd for C$_{86}$H$_{86}$N$_4$O$_4$S$_2$: C, 79.23; H, 6.65; N, 4.30. Found: C, 78.94; H, 6.65; N, 4.06.

18: a bright yellow solid after a recrystallization from DCM−ethanol; mp 133.0−133.8 °C; ^{1}H NMR (400 MHz, CDCl$_3$) δ 7.48 (d, J = 8.3 Hz, 2H), 7.36 (d, J = 8.3 Hz, 2H), 6.99 (s, 1H), 6.98 (s, 1H), 4.01 (t, J = 6.8 Hz, 2H), 4.00 (t, J = 6.8 Hz, 2H), 3.17 (t, J = 7.3 Hz, 2H), 2.63 (t, J = 7.2 Hz, 2H), 1.83 (m, 4 H), 1.52 (m, 4H), 1.36 (m, 8H), 0.91 (m, 6H); ^{13}C NMR (100 Hz, CDCl$_3$) δ 155.0, 153.5, 133.9, 132.3, 130.4, 122.6, 117.70, 117.66, 116.9, 114.8, 112.8, 94.6, 87.2, 79.5, 79.4, 69.8, 69.6, 31.6, 31.5, 29.8, 29.2, 29.1, 25.7, 25.6, 22.62, 22.58, 18.2, 14.0; λ$_{max}$ (CHCl$_3$) 276, 323, 400 nm; MS (MALDI-TOF) (m/z): 972.4 (M$^+$). Anal. Calcd for C$_{62}$H$_{72}$N$_2$O$_4$S$_2$: C, 76.50; H, 7.46; N, 2.88. Found: C, 76.34; H, 7.44; N, 2.80.

17: an orange solid after recrystallization from DCM−ethanol; mp 112.3−114.1 °C; ^{1}H NMR (400 MHz, CDCl$_3$) δ 8.75 (d, J = 5.6 Hz, 4H), 7.62 (d, J = 7.8 Hz, 2H), 7.47 (d, J = 8.5 Hz, 3H), 7.41 (d, J = 8.1 Hz, 1H), 7.35 (d, J = 8.3 Hz, 2H), 7.30 (m, 4H), 6.96 (s, 1H), 6.91 (d, J = 1.5 Hz, 1H), 6.90 (s, 1H), 6.84 (s, 1H), 4.00 (m, 4H), 3.16 (t, J = 7.2 Hz, 2H), 2.62 (t, J = 7.2 Hz, 2H), 1.81 (m, 4H), 1.52 (m, 4H), 1.35 (m, 8H), 0.89 (m, 6H); ^{13}C NMR (100 Hz, CDCl$_3$) δ 153.7, 153.6, 150.9, 148.6, 148.5, 139.9, 139.8, 139.7, 139.5, 137.8, 136.7, 136.2, 134.7, 134.2, 133.7, 132.9, 132.3, 130.4, 127.7, 123.9, 123.8, 122.7, 122.5, 121.4, 119.7, 117.7, 116.8, 113.9, 113.8, 94.9, 94.0, 92.3, 87.3, 86.8, 69.65, 69.59, 31.6, 31.5, 30.3, 29.8, 29.3, 29.2, 25.73, 25.65, 22.6, 18.2, 14.0; λ$_{max}$ (CHCl$_3$) 321, 336, 379. MS (MALDI-TOF) (m/z): 943.3 (M$^+$). Anal. Calcd for C$_{55}$H$_{50}$IN$_3$O$_2$S: C, 69.98; H, 5.34; N, 4.45. Found: C, 70.16; H, 5.42; N, 4.37.

Supporting Information Available: Copies of NMR and mass spectra; additional cyclic voltammograms and *I*−*V* data; details of self-assembly procedures, electrical characterization and theoretical studies. This material is available free of charge via the Internet at http://pubs.acs.org.

JO800120N